Agriculture, Ecosystems and Environment 364 (2024) 108882

Contents lists available at ScienceDirect

Agriculture, Ecosystems and Environment

journal homepage: www.elsevier.com/locate/agee

Long term response and adaptation of farmland water, carbon and nitrogen balances to climate change in arid to semi-arid regions

Yue Li[a,b,c,d], Michael Herbst[d], Zhijun Chen[a,b,c], Xinguo Chen[a,b,c], Xu Xu[a,b,c], Yunwu Xiong[a,b,c], Quanzhong Huang[a,b,c], Guanhua Huang[a,b,c,*]

[a] *National Key Laboratory for Efficient Utilization of Agricultural Water Resources, China Agricultural University, Beijing 100083, PR China*
[b] *Chinese-Israeli International Center for Research and Training in Agriculture, China Agricultural University, Beijing 100083, PR China*
[c] *Center for Agricultural Water Research in China, China Agricultural University, Beijing 100083, PR China*
[d] *Agrosphere (IBG-3), Forschungszentrum Jülich GmbH, Jülich 52425, Germany*

ARTICLE INFO

Keywords:
Global climate models
Rising temperature
Water-carbon-nitrogen cycles
Net ecosystem carbon budget

ABSTRACT

Climate change poses a challenge for resource utilization and environmental pollution issues caused by agricultural production, especially in arid to semi-arid regions. Farmland water, carbon and nitrogen balances are closely related to these resource and environmental issues. Thus, the Agro-Hydrological & chemical and Crop systems simulator was used to assess the response of water, carbon and nitrogen balances to climate change in a spring wheat farmland of arid to semi-arid Northwest China and to propose adaptation strategies. Five Global Climate Models from the Coupled Model Intercomparison Project 6 and two Shared Socioeconomic Pathways (SSP1–2.6 and SSP5–8.5) were used to establish scenarios with the Agro-Hydrological & chemical and Crop systems simulator to simulate farmland water, carbon and nitrogen balances for the 2025–2100 period. Various irrigation amounts and nitrogen fertilization rates were tested as compensation strategies. Results indicated that climate change could negatively affect farmland water, carbon and nitrogen balances, especially under the SSP5–8.5 scenario. Precipitation showed an increasing trend, thus percolation increased and soil water consumption decreased from 2025 to 2100. However, for the carbon budget, although the soil carbon dioxide emissions tend to decrease, the net primary production was also significantly reduced, which resulted in declining the net ecosystem carbon budget under future climatic conditions. In addition, higher temperature and increased precipitation enhanced soil inorganic nitrogen leaching and nitrous oxide emissions but reduced ammonia volatilization from 2025 to 2100. Overall, the soil total nitrogen loss was increased over time, whereas crop nitrogen uptake was significantly reduced. In relation to the SSP1–2.6 scenario, the SSP5–8.5 scenario accelerated the increase rates of soil water percolation and total nitrogen loss over time, as well as the decrease rates of crop nitrogen uptake and net primary production over time. The negative effects caused by climate change can be mitigated by reducing irrigation and increasing nitrogen fertilization. For the SSP1–2.6 scenario, 30% irrigation reduction and 30% nitrogen fertilization increase can effectively decrease soil water percolation and the related nitrogen losses while crop nitrogen uptake, net primary production and net ecosystem carbon budget increase in relation to the current management (irrigation = 240 mm and nitrogen fertilization = 200 kg ha^{-1}). For SSP5–8.5 the strategy with 45% irrigation reduction and 45% nitrogen fertilization increase can also decrease nitrogen losses and increase crop nitrogen uptake, net primary production and net ecosystem carbon budget.

1. Introduction

Globally, the farmland water, carbon and nitrogen balances have received attention because they are closely related to effective resources use and various environmental issues, e.g., soil water and fertilizer losses, groundwater pollution, greenhouse gas emissions, and ammonia (NH_3) volatilization caused by agricultural production (Tongwane and Moeletsi, 2018; Lu et al., 2019; Kamran et al., 2023). These

* Corresponding author at: National Key Laboratory for Efficient Utilization of Agricultural Water Resources, China Agricultural University, Beijing 100083, PR China

E-mail address: ghuang@cau.edu.cn (G. Huang).

https://doi.org/10.1016/j.agee.2023.108882
Received 21 August 2023; Received in revised form 25 December 2023; Accepted 31 December 2023
Available online 15 January 2024

Table 1
Detailed compensation strategies design.

Climate scenarios	Compensation strategies	Note
SSP1–2.6 SSP5–8.5	Irri$_{-15\%}$Nitr$_{+15\%}$ Irri$_{-15\%}$Nitr$_{+30\%}$ Irri$_{-15\%}$Nitr$_{+45\%}$ Irri$_{-15\%}$ Nitr$_{+60\%}$	Irri denotes irrigation strategy. The percentage means the reduced proportion of irrigation amounts compared to the current irrigation depth (i.e., 240 mm). Nitr denotes fertilization strategy. The percentage means the increased proportion of nitrogen input compared to the current nitrogen fertilization rate (i.e., 200 kg ha^{-1}).
	Irri$_{-30\%}$Nitr$_{+15\%}$ Irri$_{-30\%}$Nitr$_{+30\%}$ Irri$_{-30\%}$Nitr$_{+45\%}$ Irri$_{-30\%}$ Nitr$_{+60\%}$	
	Irri$_{-45\%}$Nitr$_{+15\%}$ Irri$_{-45\%}$Nitr$_{+30\%}$ Irri$_{-45\%}$Nitr$_{+45\%}$ Irri$_{-45\%}$ Nitr$_{+60\%}$	
	Irri$_{-60\%}$Nitr$_{+15\%}$ Irri$_{-60\%}$Nitr$_{+30\%}$ Irri$_{-60\%}$Nitr$_{+45\%}$ Irri$_{-60\%}$ Nitr$_{+60\%}$	

characteristics of water, carbon and nitrogen balances are strongly impacted by environmental changes including meteorological conditions and farmland management practices (Hatfield and Dold, 2019; Zhang et al., 2021). To mitigate these negative resource and environmental issues, many studies have assessed the response of water, carbon and nitrogen balances to environmental changes and suggested optimal field management strategies (e.g., irrigation and fertilization) over the past few decades (Riley et al., 2001; Shi et al., 2012; Patra et al., 2013; Sainju, 2019; Wang et al., 2022). However, global climate change is accelerating, such as increases in atmospheric carbon dioxide (CO_2) concentrations and temperature as well as precipitation changes (IPCC, 2014), which will significantly affect the farmland water, carbon and nitrogen dynamics (Cammarano et al., 2020). This indicates that many appropriate strategies obtained in previous studies may not adapt to future climate change, but instead have negative impacts on the sustainable development of agricultural resources and ecosystems (Habib-Ur-Rahman et al., 2022). Thus, it is highly relevant to evaluate the response of farmland water, carbon and nitrogen balances to future climate change and to propose compensation strategies for agricultural resources efficient utilization and environmental protection.

Climate change increases the uncertainty related to farmland water, carbon and nitrogen balances. Changes in precipitation, air temperature and CO_2 concentration caused by climate change can significantly affect crop growth, thereby affecting crop water consumption, nitrogen uptake and net primary production (NPP) (Chen et al., 2020; Zydelis et al., 2021). In recent years, many studies have assessed the influence of climate change on crop growth for various farmland systems and climatic zones worldwide. For example, in Northern China, some C3 and C4 crops (e.g., wheat and maize) biomass and yield are expected to decline under future climate change with increased air temperature and CO_2 concentration (Liu et al., 2020; Wang et al., 2021). In Europe, however, crop yield generally increases under future climate scenarios because the CO_2 concentration has a positive effect on crop physiological processes (Parent et al., 2018; Zydelis et al., 2021). However, due to the uncertainty of the expected crop growth and production under future climate conditions, there is considerable variation in the predicted impacts with respect to crop water consumption, nitrogen uptake and NPP (Habib-Ur-Rahman et al., 2022). Thus, assessing the response of crop water consumption, nitrogen uptake and NPP to climate change may directly support the understanding of future changes in farmland water, carbon and nitrogen balances.

Farmland water, carbon and nitrogen losses are significantly affected by climate change. Gong et al. (2013) and Tongwane and Moeletsi (2018) reported that rising temperatures may enhance soil CO_2 emissions by increasing microbial and crop root activities and may also increase soil nitrous oxide (N_2O) emissions and NH_3 volatilization by accelerating nitrification and denitrification. Changes in precipitation potentially influences soil CO_2 and N_2O emissions and NH_3 volatilization by impacting soil moisture and aeration (Scheer et al., 2012; Oertel et al., 2016). In addition, soil water percolation and inorganic nitrogen leaching are closely related to precipitation. Many studies have found that higher precipitation increased percolation, thus enhancing soil nitrogen leaching (Bouwman et al., 2005; Lu et al., 2019). However, climate change increases the uncertainty of temperature and precipitation changes in the future (Dutta et al., 2022), which complicates the prediction of water, carbon and nitrogen dynamics under future climate. How exactly fates to farmland water, carbon and nitrogen balances will evolve under different future climate conditions remains unclear.

Combining agro-hydrological and crop models with different emission scenarios of Global Climate Models (GCMs) is an effective approach to assess the influence of climate change on agricultural systems. For instance, Cammarano et al. (2020) evaluated the response of tomato water and nitrogen productivity to climate change for Italy using the DSSAT model in combination with GCMs from CMIP5 (Coupled Model Intercomparison Project 5). The response of wheat biomass and yield to climate change was estimated and appropriate field management practices were suggested for Northern China based on the SWAP model again combined with GCMs from CMIP5 (Wang et al., 2021). Tan et al. (2022) investigated the influence of climate change on water productivity and net groundwater use of winter wheat and summer maize and relevant adaptation strategies for Northwest China, based on SWAT and GCMs from CMIP6. However, these studies mainly focused on the assessment of farmland productivity and water and fertilizer utilization under future climate conditions, while little attention has been given to farmland water, carbon and nitrogen balances. Therefore, the adaptation strategies allowing to compensate negative impacts (e.g., low crop nitrogen uptake, NPP and net ecosystem carbon budget (NECB), and high soil water percolation, carbon emissions and nitrogen leaching) of climate change on farmland water, carbon and nitrogen balances are still limited. For instance, in the arid upper Yellow River basin of Northwest China, the sustainable development of agricultural resources and environmental systems is severely restricted by high water and fertilizer losses, nitrogen leaching and greenhouse gas emissions caused by excessive irrigation and nitrogen fertilization, especially in spring wheat farmland (Zhou, 2020; Li et al., 2022a). However, in the context of climate change, how these restrictions will develop in the future and how to improve irrigation and fertilization strategies to handle climate change needs to be explored.

The AHC model (Agro-Hydrological & chemical and Crop systems simulator) is an agro-hydrological model (Xu et al., 2018), which can consider the impacts of meteorological variables and atmospheric CO_2 concentration changes on farmland water, carbon, nitrogen and crop growth processes when simulation work is implemented (Liu et al., 2020). This model was also validated against experimental data and showed good performance for wheat, maize and sunflower farmlands under various irrigation, fertilization, plant density and hydrological year conditions in Northwest China, North Plain China and Northeast China (Xu et al., 2018; Huang et al., 2020; Chen et al., 2023; Li et al., 2023b; Wu et al., 2023). Thus, the AHC model was applied in this study, and the statistically downscaled daily climate data from different GCMs (CMIP6) were used as atmospheric forcing for AHC. The objectives were (1) to assess the response of spring wheat farmland water consumption, crop nitrogen uptake, NPP and NECB to future climate change in the arid to semi-arid upper Yellow River basin of Northwest China; (2) to explore the changes in soil water percolation, nitrogen losses and carbon emissions from spring wheat farmland under future climate conditions; (3) to devise appropriate compensation strategies to deal with the negative impacts of climate change on spring wheat farmland water, carbon and nitrogen balances in this region.

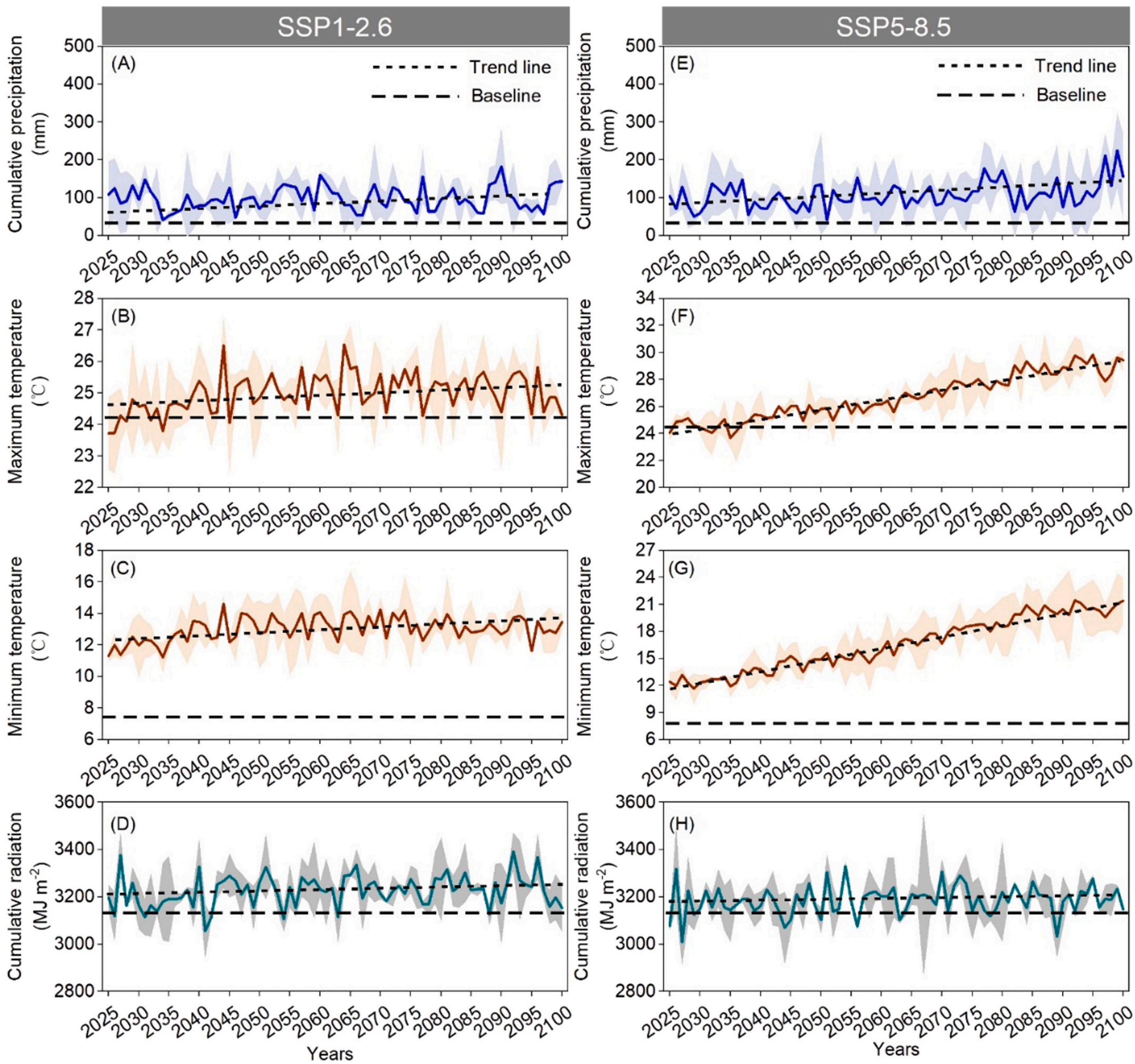

Fig. 1. Cumulative precipitation, average maximum temperature, average minimum temperature and cumulative radiation during spring wheat growing seasons under the SSP1-2.6 and SSP5-8.5 scenarios from 2025 to 2100. Note: the average values of monitored meteorological data in 2019 and 2020 was used as the meteorological baseline.

2. Materials and methods

2.1. Study site and experiment data

In the upper Yellow River basin of Northwest China (41°09′N, 107°39′E), a field experiment was carried out in 2019 and 2020. This area is dominated by arid to semi-arid temperate continental climate. Annual mean temperature and annual precipitation are in the range of 5–10℃ and 50–250 mm, respectively. Groundwater depth during the spring wheat seasons ranges between 1 and 2.8 m. Soil texture is mainly silt loam to loam and average soil depth varies around 1 m. The mean soil bulk density, organic matter, field capacity and wilting point in topsoil (0–25 cm) are 1.44 g cm^{-3}, 18.3 g kg^{-1}, 0.35 cm^3 cm^{-3} and 0.08 cm^3 cm^{-3}, in subsoil (25–100 cm) are 1.43 g cm^{-3}, 13.03 g kg^{-1}, 0.31 cm^3 cm^{-3} and 0.07 cm^3 cm^{-3}, respectively. To calibrate and validate the AHC model under different irrigation depths and nitrogen fertilization conditions, seven irrigation depth combined with nitrogen fertilization treatments [i.e., irrigation depth (mm) × nitrogen fertilization (kg ha^{-1}) = 450 × 340, 315 × 340, 180 × 340, 450 × 170, 315 × 170, 180 × 170 and 315 × 250] were considered in the experiment. Water was applied to the field by surface irrigation and fertilizer was added to the field by the broadcasting method. Three irrigations with the same amount were implemented during the tillering, jointing, and heading stages. For each treatment, 95 kg ha^{-1} phosphate, 95 kg ha^{-1} potassium and 50 kg ha^{-1} nitrogen fertilizer were applied before sowing, and then the remaining nitrogen fertilizer was applied at a ratio of 6:4 before irrigation in the tillering and jointing stages. Each treatment had three replicates, resulting in 21 test plots in total.

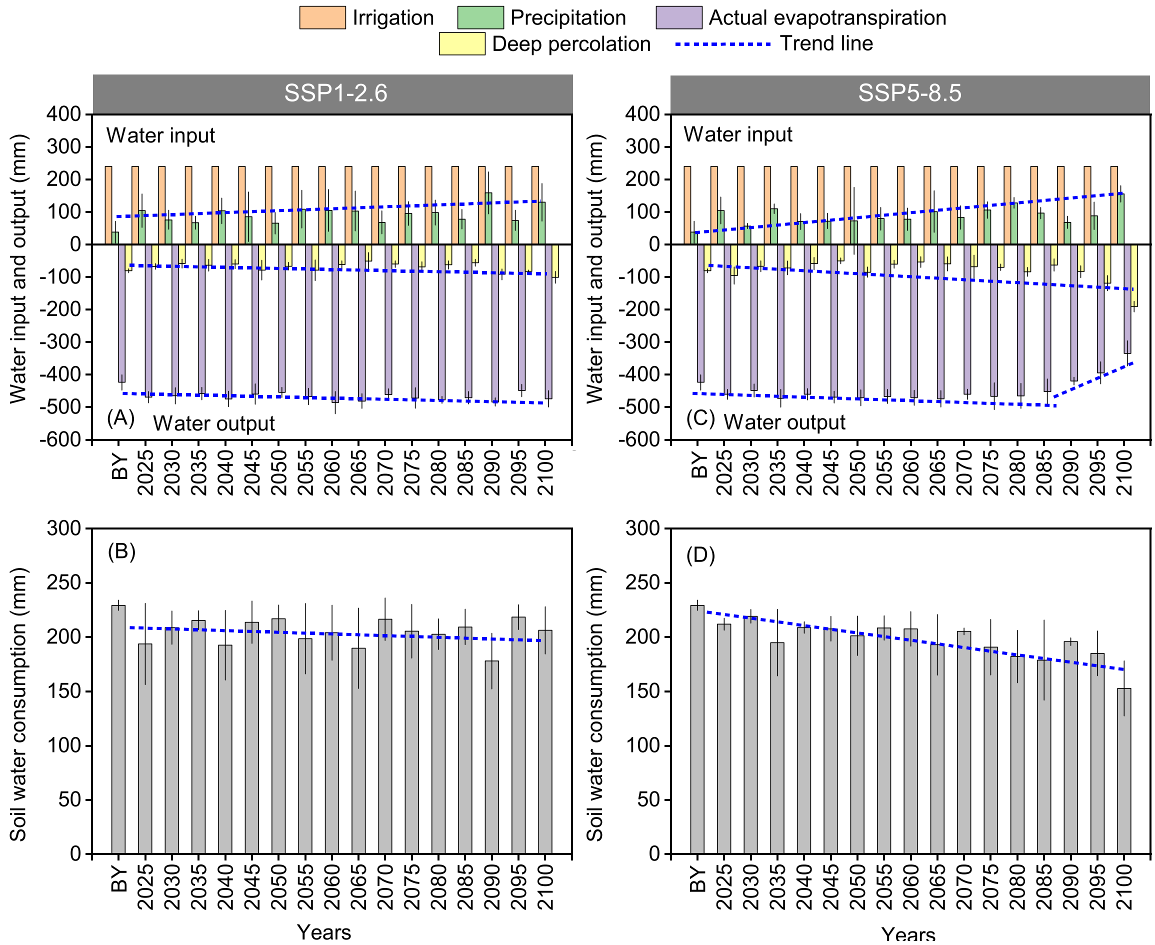

Fig. 2. Farmland water balance characteristics during spring wheat growing seasons under the SSP1-2.6 and SSP5-8.5 scenarios from 2025 to 2100. Note: BY denotes the base year. Fitting equations corresponding to each trend line are shown in Table 2.

The wheat investigated in this study was the cultivar Yongliang No. 4, and growing season covers the period from March to July in both years. The planting density was approximately 6.03×10^6 plants ha^{-1}. During the experimental period, soil water content, soil inorganic nitrogen (NH_4^+-N and NO_3^--N) concentrations, CO_2, N_2O and NH_3 fluxes, wheat leaf area index, plant height and aboveground dry biomass were measured approximately every 10 days. Soil water percolation and inorganic nitrogen leaching was measured after each irrigation or precipitation event. At harvest, undisturbed wheat plants of one square meter were harvested in the center of each test plot to measure wheat grain yield. A more detailed description of experimental design, irrigation and fertilization arrangements, soil physicochemical properties, daily meteorological and groundwater data, sample collection and test methods had been described in Li et al. (2022a); (2023b).

2.2. AHC model

The AHC is a 1-D agro-hydrological model that can simulate the transport of water, solutes and heat, mass transformation and crop growth (Xu et al., 2018). The soil water, solute and heat dynamics are simulated by the 1-D Richards' equation, convection-dispersion equation and convection-diffusion equation, respectively. The first-order reaction kinetics are used to defined carbon/nitrogen turnover processes. The source and sink terms consider soil nitrogen leaching, crop nitrogen uptake, root water extraction and nitrification and denitrification. Crop growth is described by a modified EPIC routine (Williams et al., 1989). With respect to the influence of climate change, water and temperature stress are two major factors affecting nitrification and denitrification, carbon/nitrogen turnover and crop growth. Liu et al. (2020) added the crop growth response function to atmospheric CO_2 concentration to the crop growth module. Relevant control equations can be found in Liu et al. (2020). A more detailed description of the AHC model is given by Xu et al. (2018) and Li et al. (2023b).

2.3. Model setup, calibration and validation

Soil water flow and solute transport (NH_4^+-N and NO_3^--N) were computed for a soil profile with 300 cm depth. The soil profile was divided into four horizons (i.e., 0–25 cm, 25–50 cm, 50–70 cm and 70–300 cm) according to the soil physicochemical characteristics (Table S1, see supplementary material) (Ren et al., 2016; Xu et al., 2018). Soil texture was considered as the primary basis, and other physicochemical characteristics were considered as the secondary basis. The vertical one-dimensional soil domain (0–300 cm) was discretized into 301 nodes with a uniform spacing of 1 cm. For soil water flow and solute transport, the upper and lower boundary conditions were set as the third-type (Cauchy) and first-type (Dirichlet) boundary conditions, respectively. For soil water flow, the evaporation rate and infiltration rate by precipitation and irrigation were considered as its upper boundary, while its lower boundary was defined based on the observed groundwater depth. For solute transport, the inorganic nitrogen flux introduced by precipitation and irrigation was defined as its upper boundary, while the inorganic nitrogen concentration in groundwater was defined as its lower boundary. The initial conditions for soil water flow and solute transport simulation were set based on the tested soil water and inorganic nitrogen contents before spring wheat sowing,

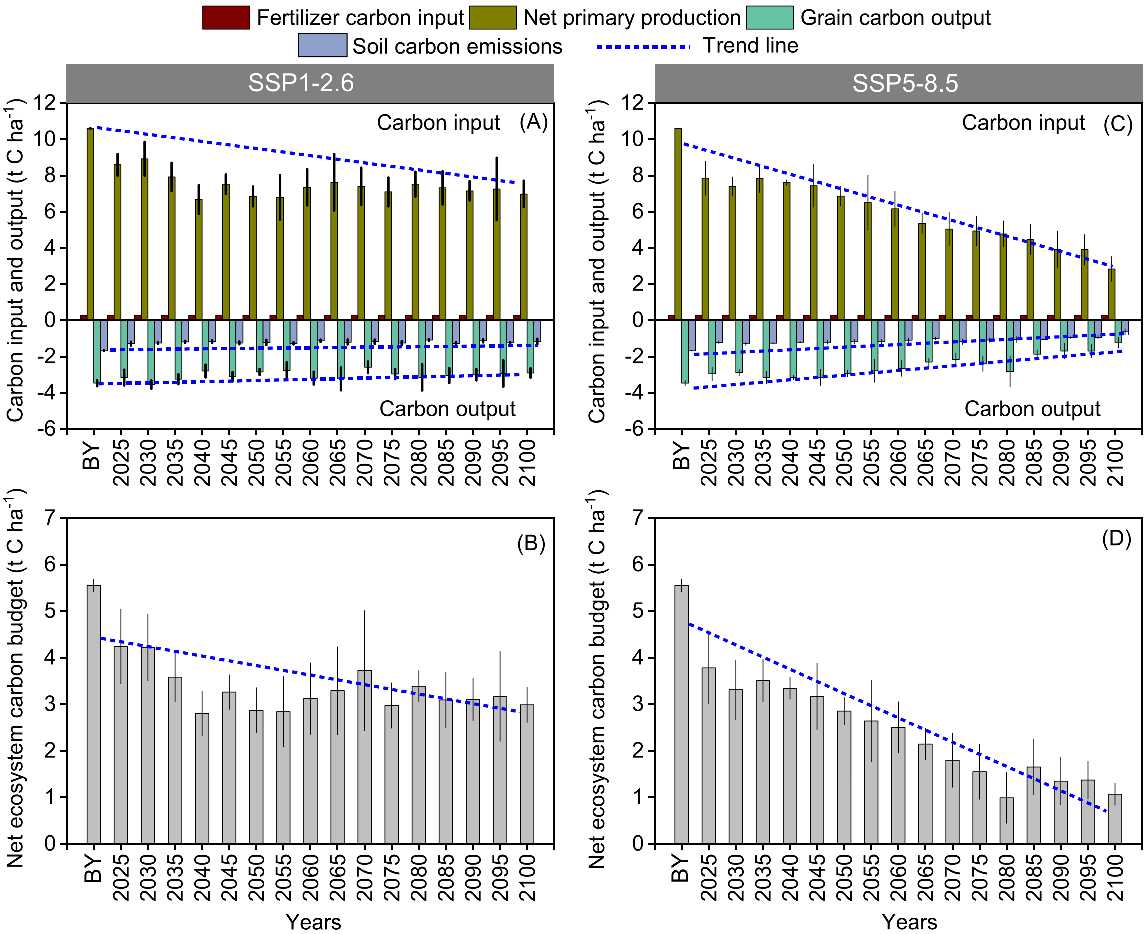

Fig. 3. Farmland carbon balance characteristics during spring wheat growing seasons under the SSP1-2.6 and SSP5-8.5 scenarios from 2025 to 2100. Note: BY denotes the base year. Fitting equations corresponding to each trend line are shown in Table 2.

respectively. The simulation period covered the full spring wheat growth period in this region.

The soil hydraulic parameters, carbon/nitrogen turnover parameters and crop growth parameters of AHC model were calibrated and validated using the measured soil water and inorganic nitrogen dynamics, water percolation and inorganic nitrogen leaching from 0−100 cm soil layers, soil CO_2, N_2O and NH_3 fluxes and crop growth indicators (leaf area index, crop height, aboveground dry biomass and grain yield) in 2019 and 2020 (Li et al., 2023b). The model performance was evaluated by comparing the results to simulations described in previous studies (Xu et al., 2018; Wang et al., 2022). The calibrated AHC model accurately captured soil water and nitrogen dynamics, water percolation, inorganic nitrogen leaching, greenhouse gas emissions, NH_3 volatilization and crop growth processes. The goodness-of-fit indices (normalized root mean square error, normalized standard error and coefficient of determination) were all in an acceptable range (Cameira et al., 2007; Zhang et al., 2012; Ren et al., 2016). The calibrated parameters and their values are shown in Table S2—**S4** (**see** supplementary material). More details on model setup, calibration and validation are given by Li et al. (2023b).

2.4. Future climate data

The CMIP6 data set was established to consider the impact of natural changes and human activities on the climate system (O'Neill et al., 2016), which brings together GCMs around the world with the goal to understand the variability and predictability of climate in the future. Therefore, meteorological data was sampled from CMIP6 in this study. To deal with these uncertainties, the future meteorological data from five GCMs was selected to drive the AHC model (Table S5 shows the basic information of these five GCMs, see Supplementary material) (Dutta et al., 2022;Tan et al., 2022). The average values of simulation results corresponding to five GCMs were calculated to reflect their responses to climate change. The standard deviations were calculated to reflect the uncertainty of simulation results, were represented by error bars. Daily meteorological data (air temperature, precipitation, solar radiation and relative humidity) of these GCMs was generated for the Linhe Meteorological Station (ID: 53513) located near the study site using a statistical downscaling method (Liu and Zuo, 2012). Each GCM from CMIP6 includes four Shared Socioeconomic Pathways (SSPs), i.e., SSP1–2.6, SSP2–4.5, SSP3–7.0 and SSP5–8.5. In this study, the SSP1–2.5 (i.e., low emission scenario) and the SSP5–8.5 (i.e., high emission scenario) were selected to assess the response of farmland water, carbon and nitrogen balances to future CO_2 emission levels. The annual atmospheric CO_2 concentration for the two SSPs from 2025 to 2100 are shown in the supplementary material (Fig. S1).

2.5. Simulation and calculation of future climate scenarios and compensation strategies design

The soil water percolation, actual evapotranspiration, inorganic nitrogen leaching, CO_2 and N_2O emissions, NH_3 volatilization, crop nitrogen uptake, crop dry biomass and grain yield were simulated under the currently recommended irrigation and fertilization strategy (i.e., irrigation depth = 240 mm and nitrogen fertilization = 200 kg ha^{-1}) (Li et al., 2023b). NPP can be calculated through multiplying the simulated

Table 2
Fitting equation corresponding to each trend line of farmland water, carbon and nitrogen balance characteristics.

SSPs	Items	Fitting equation	R^2
SSP1–2.6	Soil water percolation	y=0.91x+61.83	0.11
	ET_a	y=1.25x+454.76	0.18
	Soil water consumption	y=−0.54x+210.76	0.05
	Net primary production	y=−0.12x+8.68	0.37
	Soil CO_2 emissions	y=−0.01x+1.34	0.24
	Grain carbon output	y=−0.02x+3.26	0.23
	Net ecosystem carbon budget	y=−0.08x+4.17	0.35
	Inorganic nitrogen leaching	y=0.98x+42.80	0.57
	Soil N_2O emissions	y=0.03x+1.31	0.36
	Soil NH_3 volatilization	y=−0.12x+25.77	0.51
	Crop nitrogen uptake	y=−2.85x+236.15	0.33
SSP5–8.5	Soil water percolation	y=3.01x+52.79	0.21
	ET_a during the rising period (2025–2085)	y=2.30x+446.83	0.35
	ET_a during the decline period (2085–2100)	y=−22.5x+504.38	0.93
	Soil water consumption	y=−2.91x+224.59	0.67
	Net primary production	y=−0.37x+9.42	0.93
	Soil CO_2 emissions	y=−0.04x+1.45	0.72
	Grain carbon output	y=−0.11x+3.56	0.81
	Net ecosystem carbon budget	y=−0.22x+4.51	0.87
	Inorganic nitrogen leaching	y=4.43x+25.57	0.79
	Soil N_2O emissions	y=0.23x+0.53	0.69
	Soil NH_3 volatilization	y=−0.14x+25.69	0.45
	Crop nitrogen uptake	y=−10.28x+262	0.92

Note: x denotes the time (each time unit is 5 years). y denotes the values of each water, carbon or nitrogen characteristic. ET_a denotes the actual evapotranspiration.

crop dry biomass (including ears, leaves, stems and roots of wheat) and corresponding carbon content at harvest. The carbon removed via grain harvest can be calculated through multiplying the simulated grain yield and grain carbon content. In addition, based on these above data, the soil water storage consumption and NECB were calculated using the farmland water balance equation (Li et al., 2022a) and carbon budget equation (Chen at al., 2022; Li et al., 2023a), respectively (see supplementary material, Eqs. (S1 and S2)). The average results of 2019 and 2020 were considered as the corresponding base year results. The simulation period was 2025−2100, and the simulated output was generated every five years.

Under the influence of climate change, the precipitation and total nitrogen losses during the spring wheat growth periods showed an increasing trend from 2025 to 2100. Thus, to utilize the increased precipitation, different irrigation depth reduction strategies were designed for the future climate scenarios based on the principle of water balance. The currently recommended irrigation depth was considered as a control strategy. The maximum reduction of irrigation depth was determined based on the maximum increase of precipitation at the end of the simulation period (i.e., 2100). Moreover, considering the increase of precipitation during the different subperiods (2025–2050, 2050–2075 and 2075–2100), three irrigation strategies with lower irrigation depth reduction were added. Overall, based on the current irrigation depth (i.e., 240 mm), four irrigation reduction levels (i.e., −15%, −30%, −45% and −60%) were considered. In addition, different nitrogen fertilization increase strategies were designed as compensation strategies to deal with the increased nitrogen losses under future climate conditions. On the basis of current nitrogen fertilization rate (i.e., 200 kg ha^{-1}), four nitrogen fertilization increase levels (i.e., +15%, +30%, +45% and +60%) were considered. Under the each SSP scenario, these irrigation and fertilization treatments were completely random with sixteen combinations (Table 1). In order to obtain the appropriate compensation strategy, three future subperiods, i.e., near-term (2025–2050), mid–term (2051–2075), and long–term (2076–2100) were divided. Then, the average results of each subperiod were used to reflect the response of farmland water, carbon and nitrogen balances characteristics to different compensation strategies under the future climate conditions. In the next step, the appropriate irrigation and nitrogen fertilization compensation strategies for SSP1–2.6 and SSP5–8.5 scenarios were determined, seeking low water percolation and nitrogen losses, and high crop nitrogen uptake, NPP and NECB.

3. Results and discussion

3.1. Future climate change

Fig. 1 shows the cumulative precipitation, average maximum temperature, average minimum temperature and cumulative solar radiation during the spring wheat growing seasons from 2025 to 2100. In terms of precipitation, the SSP1–2.6 and SSP5–8.5 scenarios showed higher cumulative precipitation for the 2025–2100 period in relation to the precipitation baseline (Fig. 1A and E). From 2025–2100, the cumulative precipitation increases by 33% under the SSP1–2.6 scenario, while an even more pronounced increase by 49% was observed under the SSP5–8.5 scenario. The observed trends in average maximum and minimum temperatures over time were similar to the trends observed for precipitation (Fig. 1B, C, F and G). Again, the increase in minimum and maximum temperatures under SSP5–8.5 were higher than those under SSP1–2.6. From 2025–2100, the average maximum and minimum temperatures under SSP1–2.6 increased by 3% and 19%, while their values under SSP5–8.5 clearly increased by 23% and 73%, respectively. In contrast to precipitation and temperature, the cumulative solar radiation during the growing seasons of the both climate scenarios did not change significantly for the 2025–2100 period (Fig. 1D and H), values range between 2942 and 3470 MJ m^{-2} and between 2871 and 3548 MJ m^{-2}, respectively. These indicate that the high emission scenario describes accelerated climate warming and increased precipitation in the coming decades. The trends of the low emission scenario also indicate a temperature and precipitation increase, however at a smaller rate.

3.2. Responses of farmland water balance characteristics to future climate change

Climate change affected farmland actual evapotranspiration, soil water percolation and soil water consumption during the wheat seasons in future (Fig. 2). For the future period of 2025–2100, actual evapotranspiration gradually increased over time under SSP1–2.6, while actual evapotranspiration first increased and then decreased after 2085 under SSP5–8.5 (Fig. 2A and C). Actual evapotranspiration mainly increased because high precipitation increased the soil water storage and higher temperatures propel soil evaporation and crop transpiration (Tan et al., 2022). However, actual evapotranspiration of SSP5–8.5 scenario decreased from 2085 onwards due to excessively high temperatures during that period, resulting in a shorter growing season of spring wheat, which in turn reduced total actual evapotranspiration over wheat growing season (Rashid et al., 2019). Christy et al. (2018) and Wang et al. (2021) also reported that temperature is the main factor affecting the crop growth period, high temperature can shorten the growth period. In addition, many previous studies found that high atmospheric CO_2 concentration decreased the stomatal conductance of C3 crop (e.g., wheat), thus reducing crop transpiration (Wand et al., 1999; Gedney et al., 2006; Liu et al., 2020). This may be another reason for the actual evapotranspiration reduction under the high emission scenario in 2085–2100 period.

From the time series, the water percolation from 0–100 cm root zone soils showed a gradual increasing trend under future climate conditions (Fig. 2A and C). Water percolation slightly increased over time under the SSP1–2.6 scenario, while it clearly increased under the SSP5–8.5 scenario. In relation to base year, the water percolation in 2100 under SSP1–2.6 and SSP5–8.5 increased by 25% and 136%, respectively. The SSP1–2.6 scenario in 2100 predicted a water percolation of approximately 101 mm per season, while the SSP5–8.5 scenario in 2100

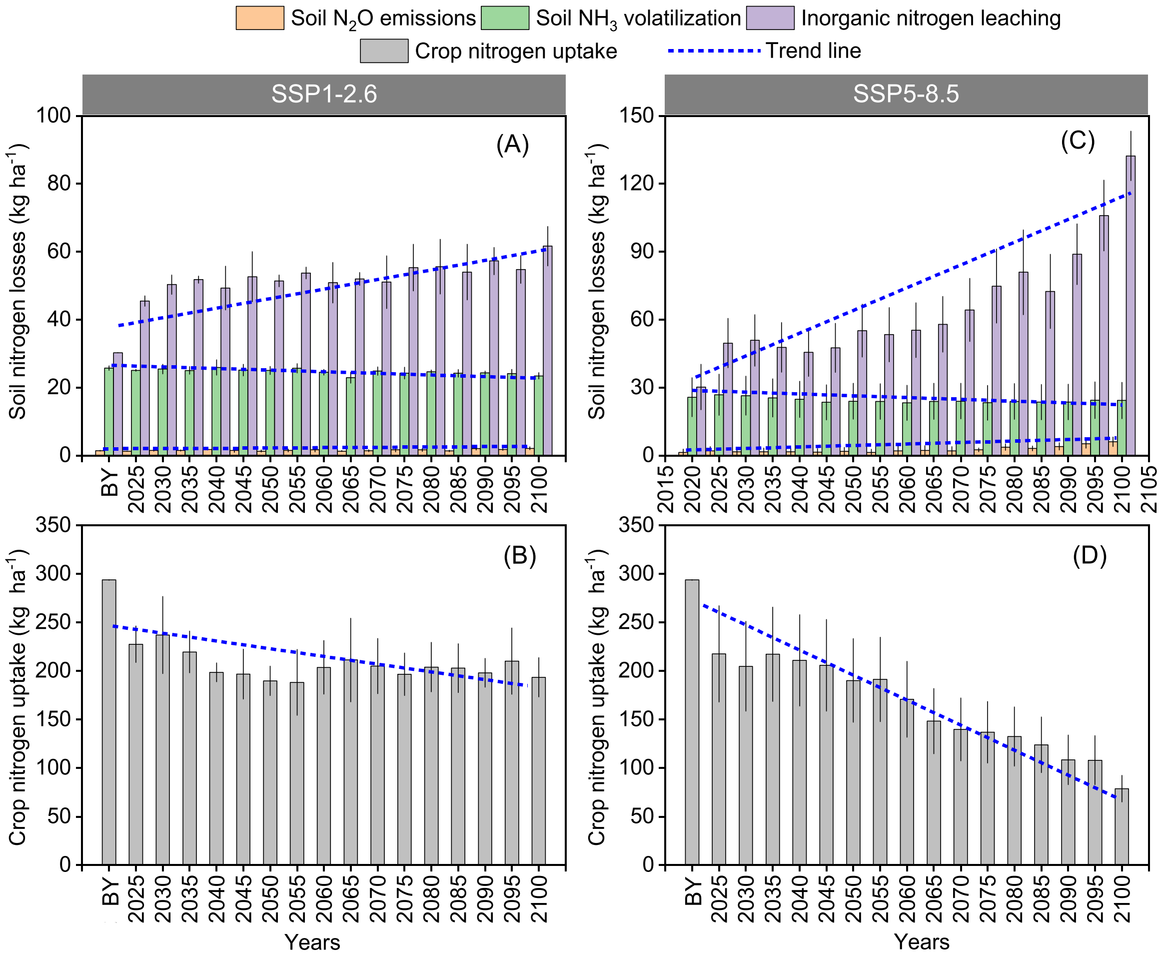

Fig. 4. Farmland nitrogen balance characteristics during spring wheat growing seasons under the SSP1-2.6 and SSP5-8.5 scenarios from 2025 to 2100. Note: BY denotes the base year. Fitting equations corresponding to each trend line are shown in Table 2.

estimated water percolation of 190 mm per season, which represents 48% of total water input (irrigation and precipitation). Because precipitation increase of the SSP5–8.5 scenario was faster than that of SSP1–2.6 scenario from 2025 to 2100, and the precipitation of SSP5–8.5 scenario was higher than the corresponding value of the SSP1–2.6 scenario. Further, the farmland water output caused by actual evapotranspiration of SSP5–8.5 scenario was lower that of the SSP1–2.6 scenario in 2085–2100 period, which further exacerbated the water percolation of the SSP5–8.5 scenario in this period. In addition, the soil water consumption decreased over time, especially under the SSP5–8.5 scenario (Fig. 2B and D). The reason for this may be that the high precipitation induced a decrease in the root water uptake rate from the soil water storage (Cammarano et al., 2020; Li et al., 2022a,b). The results indicate that although water input increased under the impact of climate change, large amounts of water cannot be stored in farmland soil and will percolate towards the groundwater, especially under the high emission scenario. These results also mean that the water use efficiency of spring wheat farmland may be reduced under the impact of future climate change, but the low emission scenario can slow down the rate of water use efficiency reduction by decreasing percolation and promoting soil water depletion compared to the high emission scenario.

3.3. Response of farmland carbon balance characteristics to future climate change

Soil CO_2 emissions showed a decreasing trend over time. The decrease was faster under the SSP5–8.5 scenario than under the SSP1–2.6 scenario (Fig. 3A and C). This is a consequence of the high precipitation causing higher soil water saturation, reducing soil aeration and available oxygen content, and finally reducing soil microbial respiration and root respiration under future climate conditions (Kamran et al., 2023; Li et al., 2020a,b). High precipitation also promoted losses of available nutrients for soil microorganisms and crop roots, thus reducing their activity and reducing respiration rates (Oertel et al., 2016; Li et al., 2023a). Precipitation under the SSP5–8.5 scenario was significantly higher than that under the SSP1–2.6 scenario. Thus, the decrease rate in CO_2 emission over time under SSP5–8.5 was faster than that under SSP1–2.6. Further, the carbon output caused by grain removal also showed a decreasing trend over time, especially under the SSP5–8.5 scenario. Overall, for the time series of 2025–2100, the total carbon output showed a decline. In relation to base year, the value of total carbon output in 2100 was smaller by 21% and by 64% under the SSP1–2.6 and the SSP5–8.5 scenario, respectively.

However, although future climate change reduced farmland total carbon output, the values of NECB were still reduced over time (Fig. 3B and D). The reduction of NECB of SSP5–8.5 scenario was significantly faster than that of SSP1–2.6 scenario. NECB decreased by approximately 0.16 t C ha^{-1} per decade for SSP1–2.6 scenario, while its value decreased by approximately 0.44 t C ha^{-1} per decade for SSP5–8.5 scenario (Fig. 3B and D, Table 2). The reason being the fact that NPP was the largest component of NECB, it determined the trend of NECB (Chen et al., 2022; Li et al., 2023a). NPP was reduced significantly over time under the impact of climate change, resulting in a reduction in NECB. Further, the SSP5–8.5 scenario induced a faster reduction in NPP in relation to the SSP1–2.6 scenario, thus this scenario caused a faster reduction in NECB. There are several possible explanations for the

Table 3
The main characteristics of farmland water, carbon and nitrogen balance for different compensation strategies under SSP1-2.6 and SSP5-8.5 scenarios in 2025−2050 period.

Compensation strategies	SSP1-2.6						SSP5-8.5					
	SWP (mm)	SWC (mm)	NPP (t C ha^{-1})	NECB (t C ha^{-1})	STNL (kg ha^{-1})	CNU (kg ha^{-1})	SWP (mm)	SWC (mm)	NPP (t C ha^{-1})	NECB (t C ha^{-1})	STNL (kg ha^{-1})	CNU (kg ha^{-1})
Irri$_{-15\%}$Nitr$_{+15\%}$	44.5 ±9.1	216.0 ±22.8	7.92±0.9	3.52±0.6	76.0±1.5	219.4 ±26.0	69.4 ±23.1	211.3 ±10.6	6.99±0.8	3.05±0.5	78.6±6.5	194.6 ±20.8
Irri$_{-15\%}$Nitr$_{+30\%}$	44.4 ±9.0	216.1 ±22.8	8.09±1.0	3.65±0.6	80.7±1.5	224.1 ±26.5	69.3 ±23.1	211.3 ±10.6	7.08±0.8	3.11±0.5	83.0±6.7	197.0 ±20.8
Irri$_{-15\%}$Nitr$_{+45\%}$	44.3 ±9.0	216.2 ±22.8	8.12±1.0	3.65±0.7	85.2±1.6	224.9 ±27.0	69.2 ±23.1	211.4 ±10.6	7.14±0.8	3.14±0.5	87.5±6.8	198.5 ±21.3
Irri$_{-15\%}$Nitr$_{+60\%}$	44.3 ±9.0	216.3 ±22.8	8.14±1.0	3.65±0.7	90.1±1.6	225.7 ±26.7	69.2 ±23.0	211.4 ±10.5	7.14±0.8	3.14±0.5	92.0±6.9	199.0 ±21.6
Irri$_{-30\%}$Nitr$_{+15\%}$	26.1 ±7.6	219.1 ±21.5	8.00±0.9	3.61±0.6	68.7±4.0	221.8 ±26.3	49.1 ±20.4	214.5 ±10.2	7.03±0.7	3.07±0.5	72.9±4.6	195.8 ±20.8
Irr$_{i-30\%}$Nitr$_{+30\%}$	26.1 ±7.6	219.2 ±21.5	8.11±1.0	3.68±0.7	73.3±4.0	224.8 ±26.7	49.1 ±20.4	214.6 ±10.1	7.14±0.7	3.16±0.5	77.4±4.9	198.3 ±21.2
Irri$_{-30\%}$Nitr$_{+45\%}$	26.0 ±7.6	219.2 ±21.5	8.15±1.0	3.68±0.7	77.8±4.1	225.7 ±26.9	49.0 ±20.3	214.6 ±10.1	7.18±0.8	3.19±0.5	81.7±5.1	199.5 ±21.6
Irri$_{-30\%}$Nitr$_{+60\%}$	25.9 ±7.6	219.2 ±21.5	8.10±1.0	3.67±0.7	82.4±4.2	224.3 ±27.4	49.0 ±20.3	214.7 ±10.1	7.19±0.8	3.19±05	86.1±5.5	200.1 ±20.2
Irri$_{-45\%}$Nitr$_{+15\%}$	12.7 ±6.2	221.3 ±20.6	7.94±0.9	3.57±0.6	62.9±4.3	220.1 ±25.4	33.3 ±16.8	217.6 ±9.5	7.22±0.8	3.28±0.5	68.3±8.2	199.6 ±21.9
Irri$_{-45\%}$Nitr$_{+30\%}$	12.7 ±6.2	221.4 ±20.5	8.06±0.9	3.65±0.6	67.3±4.4	223.3 ±25.5	33.2 ±16.7	217.7 ±9.4	7.31±0.8	3.35±0.5	72.5±8.7	201.7 ±22.2
Irri$_{-45\%}$Nitr$_{+45\%}$	12.7 ±6.2	221.4 ±20.5	8.06±1.0	3.65±0.7	71.5±4.3	223.4 ±25.3	33.2 ±16.7	217.7 ±9.4	7.35±0.8	3.38±0.5	76.8±9.2	202.8 ±22.8
Irri$_{-45\%}$Nitr$_{+60\%}$	12.6 ±6.2	221.4 ±20.5	8.08±0.9	3.64±0.7	76.1±4.5	223.8 ±24.9	33.1 ±16.7	217.8 ±9.4	7.37±0.8	3.39±0.5	81.1±9.8	203.4 ±23.1
Irri$_{-60\%}$Nitr$_{+15\%}$	5.5 ±6.6	226.8 ±18.7	7.79±0.9	3.51±0.6	59.9±5.1	215.8 ±25.6	21.9 ±12.4	220.0 ±8.3	6.99±0.7	3.09±0.4	64.9 ±11.2	194.8 ±20.5
Irri$_{-60\%}$Nitr$_{+30\%}$	5.5 ±6.5	226.9 ±18.7	7.88±0.9	3.59±0.7	64.0±5.1	218.3 ±25.2	21.9 ±12.4	220.1 ±8.3	7.07±0.8	3.16±0.4	69.0 ±11.6	196.7 ±21.1
Irri$_{-60\%}$Nitr$_{+45\%}$	5.5 ±6.5	226.9 ±18.7	7.88±1.0	3.59±0.7	68.2±5.2	218.5 ±25.4	21.9 ±12.3	220.1 ±8.2	7.11±0.8	3.19±0.5	73.2 ±12.1	197.6 ±21.6
Irri$_{-60\%}$Nitr$_{+60\%}$	5.5 ±6.5	226.9 ±18.8	7.90±1.0	3.58±0.7	72.4±5.3	218.8 ±25.3	21.8 ±12.3	220.2 ±8.2	7.11±0.8	3.21±0.5	77.3 ±12.5	198.3 ±22.0

Note: SWP, SWC, NPP, NECB, STNL and CNU denote the soil water percolation, soil water consumption, net primary production, net ecosystem carbon budget, soil total nitrogen losses and crop nitrogen uptake, respectively.

reduction of NPP: 1) High precipitation caused higher soil water saturation and waterlogging, thus reducing carbon accumulation as a consequence of reduced biomass (Igbadun et al., 2008; Li et al., 2023a); 2) High precipitation accelerated soil nutrients losses from the root zone, thereby limiting crop growth and biomass accumulation, and reducing the carbon stored in biomass (Li et al., 2022a,b). As the higher precipitation under the SSP5–8.5 scenario caused more soil water saturation, crop waterlogging and soil fertility loss, the reduction rates of NPP were significantly higher under the SSP5–8.5 scenario than that under the SSP1–2.6 scenario.

In addition to these above mechanisms caused by precipitation, temperature and CO_2 concentration can also affect NECB. The high emission scenario SSP5–8.5 estimated higher temperatures and CO_2 concentrations from 2050 to 2100. Thus, the reasons for the faster reduction of NECB for the SSP5–8.5 scenario may also include: 1) increases in temperature shortened the crop growth period, which had a negative effect on biomass accumulation and NPP (Rashid et al., 2019; Wang et al., 2021; Nawaz et al., 2022); 2) excessively high atmospheric CO_2 concentrations can result in a decrease of stomatal conductance (particularly C3 crops), thereby reducing carbon fixation rate by limiting crop photosynthesis (Wand et al., 1999; Liu et al., 2020). The results show that future climate change will negatively affect NECB, especially under the high emission scenario. High precipitation, soil fertility loss, temperature and CO_2 concentration are the main reasons for the reduction of NECB under the high emission scenario, while NECB under the low emission scenario is mainly restricted by high precipitation and soil fertility loss.

3.4. Response of soil nitrogen balance characteristics to future climate change

Soil inorganic nitrogen leaching, N_2O emission and NH_3 volatilization are the main pathways of farmland nitrogen losses (Bedada et al., 2016; Zhang et al., 2021), which are significantly affected by climate change (Fig. 4A and C). Soil inorganic nitrogen leaching and N_2O emissions during the spring wheat growing seasons both showed continuous and significantly increasing trends under the SSP5–8.5 scenario, with an increase of 8.86 and 0.46 kg ha^{-1} per decade, respectively. For SSP1–2.6 scenario, nitrogen leaching and N_2O emissions slightly increased over time and reached about 1.96 and 0.06 kg ha^{-1} per decade, respectively, representing 22% and 13% of the losses estimated for the SSP-8.5 scenario (Fig. 4A and C, Table 2). Because water percolation showed an increasing trend over time, resulting in large quantities of NO_3^--N and NH_4^+-N leaching out the top 1 m of the soils, especially under the high emission scenario. The increase of the soil N_2O emissions from 2025 to 2100 can be explained by higher soil water saturation, caused by higher precipitation, increasingly generating more anaerobic conditions for nitrification and denitrification bacteria (Scheer et al., 2012; Butterbach-Bahl et al., 2013). Further, high temperatures improve the activity of nitrification and denitrification bacteria (Bouwman et al., 2005; Hayakawa et al., 2009), thus increasing soil N_2O emissions.

However, unlike nitrogen leaching and N_2O emissions, soil NH_3 volatilization was reduced under the impact of climate change (Fig. 4A and C). The reason for this result may be that the increased precipitation led to higher soil moisture, which caused more NH_3 was dissolved and ultimately reduced soil NH_3 volatilization over time (Yang et al., 2019).

Table 4
The main characteristics of farmland water, carbon and nitrogen balance for different compensation strategies under SSP1-2.6 and SSP5-8.5 scenarios in 2051−2075 period.

Compensation strategies	SSP1-2.6						SSP5-8.5					
	SWP (mm)	SWC (mm)	NPP (t C ha^{-1})	NECB (t C ha^{-1})	STNL (kg ha^{-1})	CNU (kg ha^{-1})	SWP (mm)	SWC (mm)	NPP (t C ha^{-1})	NECB (t C ha^{-1})	STNL (kg ha^{-1})	CNU (kg ha^{-1})
$Irri_{-15\%}Nitr_{+15\%}$	60.8 ±13.6	213.3 ±22.4	7.21±0.8	3.07±0.5	77.5±4.8	207.4 ±22.5	54.7 ±18.4	203.8 ±21.0	6.31±1.1	2.62±0.6	93.2±9.8	175.8 ±30.3
$Irri_{-15\%}Nitr_{+30\%}$	60.7 ±13.6	213.5 ±22.4	7.31±0.8	3.14±0.5	82.1±5.0	210.1 ±23.2	54.6 ±18.4	203.7 ±21.0	6.36±1.1	2.67±0.6	97.9±9.7	177.1 ±29.7
Irri-15%$Nitr_{+45\%}$	60.7 ±13.6	213.5 ±22.4	7.37±0.8	3.17±0.5	86.7±5.2	211.6 ±23.5	54.5 ±18.4	203.8 ±21.1	6.38±1.1	2.70±0.6	102.7 ±9.6	177.7 ±29.8
$Irri_{-15\%}Nitr_{+60\%}$	60.6 ±13.6	213.6 ±22.4	7.42±0.9	3.20±0.5	91.4±5.4	212.8 ±23.9	54.5 ±18.4	203.8 ±21.0	6.37±1.1	2.68±0.6	107.6 ±9.5	177.5 ±29.7
$Irri_{-30\%}Nitr_{+15\%}$	40.4 ±11.8	216.6 ±21.7	7.26±0.8	3.11±0.5	71.2±6.6	208.5 ±22.6	35.8 ±15.9	207.2 ±21.1	6.31±1.1	2.63±0.6	85.9±6.9	175.8 ±29.6
$Irr_{i-30\%}Nitr_{+30\%}$	40.3 ±11.8	216.8 ±21.7	7.34±0.8	3.16±0.5	73.8±6.8	210.7 ±23.1	35.8 ±15.8	207.2 ±21.1	6.38±1.1	2.71±0.6	90.5±7.0	177.4 ±29.6
$Irri_{-30\%}Nitr_{+45\%}$	40.2 ±11.8	216.9 ±21.6	7.40±0.9	3.20±0.5	80.1±7.1	212.1 ±23.6	35.8 ±15.8	207.2 ±21.1	6.40±1.1	2.72±0.6	95.2±7.0	177.9 ±29.6
$Irri_{-30\%}Nitr_{+60\%}$	40.2 ±11.8	216.9 ±21.6	7.44±0.9	3.22±0.5	84.6±7.3	213.1 ±23.9	35.7 ±15.8	207.3 ±21.0	6.39±1.1	2.72±0.6	100.0 ±7.2	177.4 ±29.6
$Irri_{-45\%}Nitr_{+15\%}$	24.1 ±9.5	219.3 ±20.9	7.16±0.8	3.04±0.5	66.2±5.9	206.6 ±23.1	21.9 ±12.8	210.2 ±20.5	6.46±1.1	2.81±0.6	78.2±8.4	178.3 ±30.0
$Irri_{-45\%}Nitr_{+30\%}$	24.1 ±9.5	219.4 ±20.9	7.22±0.9	3.08±0.5	70.4±6.1	208.6 ±20.4	21.8 ±12.8	210.2 ±20.5	6.52±1.1	2.87±0.6	82.7±8.7	179.7 ±29.8
$Irri_{-45\%}Nitr_{+45\%}$	24.0 ±9.5	219.4 ±20.8	7.26±0.9	3.09±0.5	74.7±6.3	209.2 ±24.1	21.8 ±12.7	210.2 ±20.4	6.53±1.1	2.89±0.6	87.3±9.0	180.1 ±29.9
$Irri_{-45\%}Nitr_{+60\%}$	24.0 ±9.5	219.5 ±20.8	7.29±0.9	3.11±0.5	79.1±6.4	209.9 ±24.3	21.8 ±12.7	210.2 ±20.4	6.53±1.1	2.90±0.6	91.9±9.4	180.2 ±29.2
$Irri_{-60\%}Nitr_{+15\%}$	12.6 ±6.8	220.9 ±20.2	6.99±0.8	2.97±0.5	63.5±6.1	202.3 ±24.7	12.4 ±9.6	212.4 ±19.0	6.16±1.0	2.60±0.5	71.4±6.7	171.8 ±27.1
$Irri_{-60\%}Nitr_{+30\%}$	12.6 ±6.7	221.0 ±20.2	7.05±0.8	3.01±0.5	67.5±6.3	203.7 ±23.2	12.4 ±9.6	212.4 ±19.0	6.22±1.0	2.66±0.5	75.8±6.9	173.0 ±27.2
$Irri_{-60\%}Nitr_{+45\%}$	12.6 ±6.7	221.0 ±20.2	7.08±0.8	3.02±0.5	71.7±6.5	204.4 ±23.4	12.4 ±9.6	212.3 ±19.0	6.23±1.0	2.67±0.5	80.2±7.1	173.4 ±27.3
$Irri_{-60\%}Nitr_{+60\%}$	12.6 ±6.7	221.0 ±20.2	7.11±0.9	3.05±0.5	75.9±8.6	205.1 ±23.7	12.4 ±9.6	212.4 ±18.9	6.25±1.0	2.69±0.5	84.7±7.3	173.7 ±27.4

Note: the abbreviations for variable names are the same as those described in Table 3.

Moreover, the substrate (i.e., NH_4^+-N) for NH_3 volatilization in topsoil decreased due to the accelerated leaching, nitrification and denitrification (Liu et al., 2017). Furthermore, the SSP1–2.6 scenario shows a slower increase in precipitation and temperature in relation to the SSP5–8.5 scenario. Thus, the increase of nitrogen leaching and N_2O emissions and the decline of the NH_3 volatilization rate over time was slower under SSP1–2.6 than under SSP5–8.5. Generally, the total soil nitrogen loss showed an increasing trend under future climate conditions, but for the lower emission scenario lower total nitrogen loss over time were estimated. Total nitrogen loss of SSP1–2.6 scenario in 2100 increased by 52%, in relation to the base year, while the loss of SSP5–8.5 scenario in 2100 increased by 183%. The results indicate that future climate change will increase the risk of groundwater and atmosphere pollution caused by farmland soil nitrogen losses.

In contrast to soil total nitrogen loss, crop nitrogen uptake showed a decreasing trend over time. The decrease rate was faster under SSP5–8.5 than that under SSP1–2.6 (Fig. 4B and D). The estimated decrease of nitrogen uptake was 5.7 kg ha^{-1} per decade (Table 2), from 236.3 kg ha^{-1} in 2025–193.5 kg ha^{-1} in 2100 for the SSP1–2.6 scenario. Approximately 20.6 kg ha^{-1} per decade (Table 2), from 233.3 kg ha^{-1} in 2025–78.8 kg ha^{-1} in 2100, were lost using the SSP5–8.5 scenario. Since crop nitrogen uptake was impacted by crop growth and biomass accumulation, the reason for the decrease in nitrogen uptake over time was the same as for the decrease in NPP over time, i.e., for the SSP1–2.6 scenario, high precipitation and high soil fertility loss were the main impacting factors of nitrogen uptake reduction. Whereas, for the SSP5–8.5 scenario, the impacting factors also include nitrogen uptake reduction as a consequence of higher temperatures combined with higher CO_2 concentrations.

3.5. *Compensation strategies for future climate change*

Soil water percolation, water consumption, total nitrogen loss, crop nitrogen uptake, NPP and NECB under future climate scenarios in three subperiods, i.e., 2025–2050, 2051–2075 and 2076–2100 are shown in Table 3–5. Regardless of the climate scenarios, reducing irrigation decreased water percolation and increased soil water consumption from 2025 to 2100, suggesting that water use efficiency would be improved by reducing future irrigation. In addition, reducing irrigation decreased soil total nitrogen loss over the 2025–2100 period, and the increase rate of total nitrogen loss was clearly slowed down. For example, under the same fertilization conditions, compared with the $Irri_{-15\%}$ irrigation strategy, the $Irri_{-50\%}$ irrigation strategy reduced total nitrogen loss by 9–21% and 16–23% for the 2025–2100 period under SSP1–2.6 and SSP5–8.5 scenarios, respectively (Table 3–5). Because reducing irrigation water input caused lower percolation, less NO_3-N and NH_4^+-N leached out of root zone soil (Riley et al., 2001; Salo and Turtola, 2006). Reducing irrigation also decreased soil water saturation and reduced the periods with anaerobic conditions in the soil, thereby significantly reducing soil N_2O emissions as a consequence of decreased nitrification and denitrification rates (Scheer et al., 2012; Trost et al., 2016).

However, for crop nitrogen uptake and NPP, their values initially increased and then decreased with the decrease of irrigation. The $Irri_{-30\%}$ strategy with 168 mm irrigation and the $Irri_{-45\%}$ strategy with 132 mm irrigation showed the highest values for the SSP1–2.6 and SSP5–8.5 scenarios in all three future subperiods, respectively. The reason is that properly adjusted irrigation could promote crop growth and increase crop carbon and nitrogen fixation by mitigating crop waterlogging and soil nutrient losses (Zhang et al., 2017; Zhou, 2020), while excessively reduced irrigation might provoke a soil water deficit and limit crop

Table 5
The main characteristics of farmland water, carbon and nitrogen balance for different compensation strategies under SSP1-2.6 and SSP5-8.5 scenarios in 2076−2100 period.

Compensation strategies	SSP1-2.6						SSP5-8.5					
	SWP (mm)	SWC (mm)	NPP (t C ha^{-1})	NECB (t C ha^{-1})	STNL (kg ha^{-1})	CNU (kg ha^{-1})	SWP (mm)	SWC (mm)	NPP (t C ha^{-1})	NECB (t C ha^{-1})	STNL (kg ha^{-1})	CNU (kg ha^{-1})
$Irri_{-15\%}Nitr_{+15\%}$	45.4 ±11.0	218.6 ±17.1	7.15±0.7	3.01±0.5	82.0±5.2	202.1 ±19.2	106.8 ±35.6	187.8 ±21.6	4.39±0.6	1.79±0.4	112.5 ±29.8	121.6 ±17.2
$Irri_{-15\%}Nitr_{+30\%}$	45.4 ±11.0	218.7 ±17.2	7.30±0.7	3.13±0.5	86.1±5.4	206.3 ±19.6	106.8 ±35.6	187.7 ±21.6	4.40±0.6	1.81±0.4	116.9 ±30.0	122.0 ±17.2
$Irri_{-15\%}Nitr_{+45\%}$	45.3 ±11.0	218.8 ±17.1	7.30±0.7	3.11±0.5	90.1±5.7	206.3 ±20.0	106.8 ±35.6	187.8 ±21.6	4.42±0.6	1.83±0.4	121.2 ±30.3	122.4 ±17.3
$Irri_{-15\%}Nitr_{+60\%}$	45.2 ±11.0	218.8 ±17.2	7.32±0.7	3.12±0.5	94.1±6.1	206.9 ±19.9	106.8 ±35.6	187.8 ±21.6	4.43±0.6	1.85±0.4	125.6 ±30.5	122.7 ±17.3
$Irri_{-30\%}Nitr_{+15\%}$	27.4 ±9.6	221.8 ±16.4	7.21±0.7	3.08±0.5	73.3±7.0	203.7 ±19.1	80.6 ±33.8	190.1 ±21.9	4.39±0.6	1.80±0.4	103.9 ±27.9	121.7 ±16.9
$Irr_{i-30\%}Nitr_{+30\%}$	27.3 ±9.6	221.9 ±16.5	7.30±0.7	3.14±0.5	75.4±7.5	206.4 ±19.5	80.6 ±33.8	190.1 ±22.0	4.41±0.6	1.82±0.4	108.1 ±28.1	122.1 ±17.0
$Irri_{-30\%}Nitr_{+45\%}$	27.2 ±9.6	221.9 ±16.5	7.31±0.7	3.13±0.5	81.1±8.0	206.6 ±19.6	80.6 ±33.8	190.1 ±21.9	4.42±0.6	1.84±0.4	112.4 ±28.4	122.4 ±17.0
$Irri_{-30\%}Nitr_{+60\%}$	27.1 ±9.6	222.0 ±16.5	7.33±0.7	3.14±0.5	85.2±8.5	207.1 ±19.7	80.6 ±33.8	190.1 ±21.9	4.42±0.6	1.85±0.4	116.7 ±28.6	122.6 ±17.0
$Irri_{-45\%}Nitr_{+15\%}$	14.1 ±7.7	224.1 ±16.0	7.12±0.6	2.98±0.5	67.8±8.9	201.5 ±20.1	57.7 ±31.4	192.4 ±22.1	4.38±0.6	1.80±0.3	95.3 ±25.1	121.4 ±16.3
$Irri_{-45\%}Nitr_{+30\%}$	14.0 ±7.7	224.2 ±16.0	7.23±0.7	3.07±0.5	71.6±9.4	204.8 ±20.5	57.7 ±31.4	192.4 ±22.1	4.39±0.6	1.82±0.3	99.4 ±25.3	121.7 ±16.4
$Irri_{-45\%}Nitr_{+45\%}$	14.0 ±7.7	224.2 ±16.0	7.23±0.7	3.05±0.5	75.5±9.9	204.7 ±21.0	57.7 ±31.4	192.4 ±22.1	4.40±0.6	1.83±0.3	103.6 ±25.5	121.9 ±16.4
$Irri_{-45\%}Nitr_{+60\%}$	14.0 ±7.7	224.2 ±16.0	7.25±0.7	3.06±0.5	79.4 ±10.4	205.2 ±21.1	57.7 ±31.4	192.4 ±22.1	4.40±0.6	1.85±0.3	107.7 ±25.7	122.0 ±16.4
$Irri_{-60\%}Nitr_{+15\%}$	6.8 ±6.8	229.6 ±14.4	6.91±0.7	2.90±0.6	64.4±9.6	196.6 ±20.8	38.4 ±28.8	194.6 ±21.9	4.32±0.6	1.78±0.3	87.4 ±19.3	119.7 ±15.2
$Irri_{-60\%}Nitr_{+30\%}$	6.8 ±6.7	229.7 ±14.4	7.01±0.7	2.98±0.6	68.0 ±10.1	199.3 ±20.9	38.4 ±28.8	194.6 ±21.9	4.33±0.6	1.80±0.3	91.3 ±19.4	120.0 ±15.3
$Irri_{-60\%}Nitr_{+45\%}$	6.8 ±6.7	229.7 ±14.4	7.01±0.7	2.97±0.6	71.8 ±10.6	199.4 ±21.4	38.4 ±28.8	194.6 ±21.9	4.33±0.6	1.81±0.3	95.3 ±19.5	120.1 ±15.3
$Irri_{-60\%}Nitr_{+60\%}$	6.7 ±6.7	229.7 ±14.5	7.02±0.7	2.98±0.6	75.5 ±11.0	199.7 ±21.5	38.4 ±28.8	194.6 ±21.9	4.34±0.6	1.83±0.3	99.4 ±19.6	120.2 ±15.3

Note: the abbreviations for variable names are the same as those described in Table 3.

production (Li et al., 2022a). Moreover, the SSP5–8.5 scenario caused higher increase in precipitation in relation to the SSP1–2.6 scenario. Thus, the appropriate irrigation of SSP5–8.5 scenario was lower than that of SSP1–2.6 scenario. Due to the impact of NPP, NECB also showed a trend of increasing initially and then decreasing as irrigation decreased. The highest NECB was obtained for the $Irri_{-30\%}$ and the $Irri_{-45\%}$ irrigation strategies under the SSP1–2.6 and the SSP5–8.5 scenarios in 2025–2100 period, respectively. These results indicate that 168 mm per season and 132 mm per season of irrigation are appropriate irrigation compensation strategies for future low emission and high emission scenarios, respectively.

Increasing nitrogen fertilizer input appropriately can supply soil nitrogen pools to deal with nitrogen losses during the crop growth season, thus promoting crop growth and biomass accumulation, and also increasing nutrient absorption (Mon et al., 2016; Li et al., 2022a, 2023a). This study observed that the crop nitrogen uptake, NPP and NECB showed increasing trends with increased nitrogen fertilization for the SSP1–2.6 scenario over the 2025–2100 period. Excessive nitrogen fertilization was ineffective and significantly enhanced soil nitrogen losses. The $Nitr_{+30\%}$ nitrogen fertilization strategy could ensure relatively high crop nitrogen uptake, NPP and NECB in combination with low soil total nitrogen loss (Table 3–5). For the SSP5–8.5 scenario positive nitrogen fertilization effects on these indicators were also observed from 2025 to 2100. Increasing nitrogen fertilization from 230 kg ha^{-1} ($Nitr_{+15\%}$) to 290 kg ha^{-1} ($Nitr_{+45\%}$) improved these indicators, while continuously increasing nitrogen input from 290 kg ha^{-1} to 320 kg ha^{-1} ($Nitr_{+60\%}$) did not provide an improvement. This might be related to the fact that the high nitrogen input exceeded the maximum crop nitrogen demand (Shi et al., 2012; Mon et al., 2016). In addition, under the SSP5–8.5 scenario, the change rate of these indicators was significantly lower for the 2076–2100 period than that for the 2025–2075 period. The reason might be that on the one hand the wheat was subjected to severe heat stress for the 2076–2100 period, thus limiting nitrogen uptake rates (Christy et al., 2018; Nawaz et al., 2022). On the other hand, high CO_2 concentration decreased the stomatal conductance of wheat leaves, thereby reducing the carbon fixation rate by photosynthesis (Wand et al., 1999; Liu et al., 2020).

Considering the interactive effects of irrigation and nitrogen fertilization, under the low emission scenario, the compensation strategies with 168 mm irrigation and 260 kg ha^{-1} nitrogen fertilization per season ($Irri_{-30\%}Nitr_{+30\%}$) are recommended for spring wheat in study region from 2025 to 2100. Whereas, under the high emission scenario, the compensation strategies with 132 mm irrigation and 290 kg ha^{-1} nitrogen fertilization per season ($Irri_{-45\%}Nitr_{+45\%}$) are recommended. From 2025 to 2100, compared with the current irrigation and fertilization strategy, the recommended compensation strategy reduced water percolation and total soil nitrogen loss by 48–61% and –4–17%, and increased soil water consumption, crop nitrogen uptake, NPP and NECB by 3–12%, 3–13%, 3–13% and 4–19% under the low emission scenario (Fig. 5A). For the high emission scenario, the recommended compensation strategy reduced water percolation and total nitrogen loss by 45–80% and 3–32%, and increased soil water consumption, crop nitrogen uptake, NPP and NECB by 5–9%, 3–9%, 3–9% and 6–20% compared to the current strategy (Fig. 5B), respectively. These results demonstrate that the negative effects of future climate change on farmland water, carbon and nitrogen balances can be mitigated by reducing irrigation and increasing nitrogen fertilization.

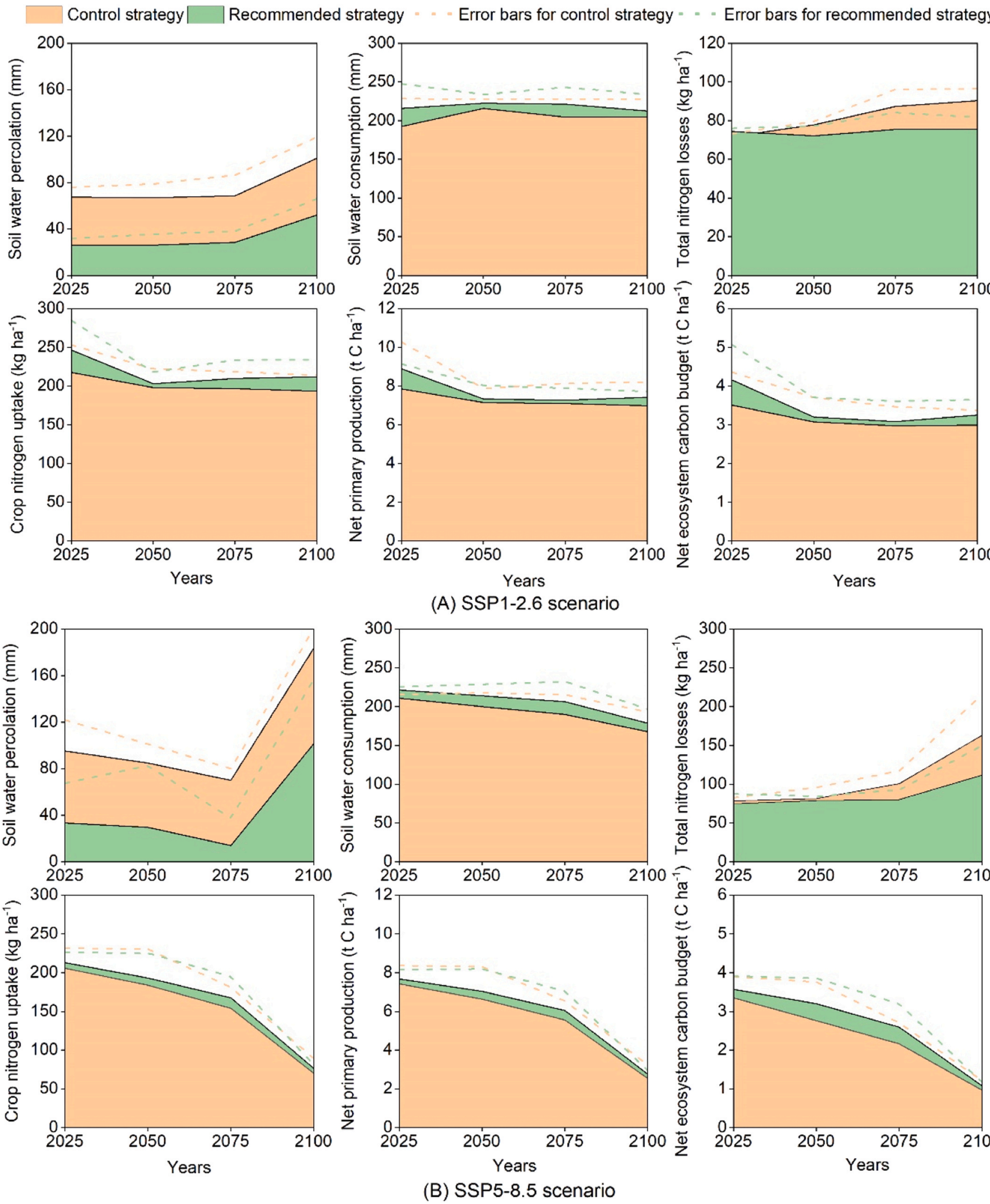

Fig. 5. Comparison between control strategy and recommended strategy under SSP1-2.6 and SSP5-8.5 scenarios.

3.6. Limitations and suggestions

Although this study assessed the responses of farmland water, carbon and nitrogen balances to climate change and proposed appropriate compensation strategies in arid to semi-arid regions, there are still certain limitations. On one hand, crop nitrogen uptake, NPP and NECB of these recommended compensation strategies for the 2025–2100 period are still lower than for the base year, indicating that the negative effects caused by future high temperatures and high CO_2 concentrations cannot be completely offset by improving irrigation depth and nitrogen fertilization rate (Wang et al., 2021; Habib-Ur-Rahman et al., 2022). The main reason may be that the current wheat varieties are not adapted to the future environmental conditions with high temperatures and high CO_2 concentrations. More compensation strategies should be considered in addition to improving irrigation depth and nitrogen fertilization, such as adjusting plant density, irrigation dates and times. Changes in atmospheric CO_2 concentration and temperature in the future may result in current plant density not being suitable for wheat production in this region (Chen et al., 2023). Furthermore, climate change will probably affect the phenological development of spring wheat, requiring adjusted irrigation dates and times (Wang et al., 2021; Huang et al., 2022).

On the other hand, appropriate compensation strategies are closely related to the specific climate and soil conditions. The farmers growing wheat all over the world on different soils will face various challenges with respect to the various levels of climate change impacts. Therefore, another limitation is that the compensation strategies (i.e., irrigation depths and nitrogen fertilization rates) proposed in this study are to a certain degree specific to this region and regions with similar conditions. Nevertheless, this study provided an effective method for determining appropriate irrigation depth and nitrogen fertilization compensation strategies under future climate conditions in various soil and climate regions. Taking into account the limitations above, future work should focus on three aspects: 1) considering more field management compensation strategies (e.g., adjusting planting density, irrigation dates and times) for spring wheat farmland to adapt to future climate change; 2) searching for new wheat varieties that are better adapted to high temperature and high CO_2 concentrations and replacing the wheat varieties currently grown in the region with new varieties to deal with the potentially negative impacts of future climate change on agro-ecosystem; and 3) determining appropriate irrigation depth and nitrogen fertilization compensation strategies for spring wheat farmland under future climate conditions in regions with different soil and climate conditions worldwide.

4. Conclusions

This study combined the AHC model with future climate models to quantify and assess the response of water, carbon and nitrogen balances to climate change in a spring wheat farmland of arid to semi-arid region and to propose adaptation strategies. The results indicated that precipitation shows an increasing trend, thus percolation increased and soil water consumption decreased from 2025 to 2100. In addition, future climate change reduced farmland total carbon output, but the net ecosystem carbon budget was still reduced over time as the net primary production was significantly reduced. Climate change also significantly reduced crop nitrogen uptake and enhanced soil total nitrogen loss. The change rates in percolation, soil water consumption, soil nitrogen loss, crop nitrogen uptake, net primary production, and net ecosystem carbon budget over time under the SSP5–8.5 scenario were faster than that under the SSP1–2.6 scenario. High precipitation, soil fertility loss, temperature and CO_2 concentration are the main reasons for the decrease in crop nitrogen uptake and net primary production under SSP5–8.5, while the crop nitrogen uptake and net primary production under SSP1–2.6 is mainly restricted by high precipitation and soil fertility loss. Reducing irrigation and increasing nitrogen fertilization can mitigate the negative effects of climate change on farmland water, carbon and nitrogen balances to some extent, but these negative effects cannot be completely offset by adjusting irrigation and fertilization management. Optimizing planting density, adjusting irrigation dates and times, and developing wheat varieties that are resistant to high temperatures and high CO_2 concentrations may be the potential ways to address these negative impacts caused by future climate change.

CRediT authorship contribution statement

Yue Li: Writing – review & editing, Writing – original draft, Methodology, Investigation, Formal analysis, Data curation. **Michael Herbst:** Writing – review & editing, Methodology, Conceptualization. **Zhijun Chen:** Methodology, Investigation. **Xinguo Chen:** Resources, Data curation. **Xu Xu:** Software, Methodology. **Yunwu Xiong:** Investigation, Conceptualization. **Quanzhong Huang:** Resources, Conceptualization. **Guanhua Huang:** Writing – review & editing, Supervision, Resources, Conceptualization.

Declaration of Competing Interest

The authors declare that they have no known competing financial interests or personal relationships that could have appeared to influence the work reported in this paper.

Data availability

The authors do not have permission to share data.

Acknowledgments

This research was jointly supported by National Natural Science Foundation of China (with numbers: 52220105007, U2243217 and 52022108) and the Key Research Project of Science and Technology in Inner Mongolia Autonomous Region of China (with numbers: NMKJXM202004 and NMKJXM202208-2). We also acknowledge Researcher Deli Liu from Wagga Wagga Agricultural Institute, Australia for his help in providing the statistical downscale meteorological data from CMIP6.

Appendix A. Supporting information

Supplementary data associated with this article can be found in the online version at doi:10.1016/j.agee.2023.108882.

References

Bedada, W., Lemenih, M., Karltun, E., 2016. Soil nutrient build-up, input interaction effects and plot level N and P balances under long-term addition of compost and NP fertilizer. Agric. Ecosyst. Environ. 218, 220–231.

Bouwman, A.F., Drecht, G.V., Hoek, K.Wvd, 2005. Surface N balances and reactive N loss to the environment from global intensive agricultural production systems for the period 1970-2030. Sci. China Ser. C. Life Sci. 48, 767–779.

Butterbach-Bahl, K., Baggs, E.M., Dannenmann, M., Kiese, R., Zechmeister-Boltenstern, S., 2013. Nitrous oxide emissions from soils: how well do we understand the processes and their controls? Philos. Trans. Biol. Sci. 368, 1–13.

Cameira, M.R., Fernando, R.M., Ahuja, L.R., Ma, L., 2007. Using RZWQM to simulate the fate of nitrogen in field soil–crop environment in the Mediterranean region. Agric. Water Manag. 90 (1-2), 121–136.

Cammarano, D., Ronga, D., Mola, I.D., Mori, M., Parisi, M., 2020. Impact of climate change on water and nitrogen use efficiencies of processing tomato cultivated in Italy. Agric. Water Manag. 241, 106336.

Chen, P., Yang, J., Jiang, Z., Zhu, E., Mo, C., 2020. Prediction of future carbon footprint and ecosystem service value of carbon sequestration response to nitrogen fertilizer rates in rice production. Sci. Total Environ. 735, 139506.

Chen, Z., Huang, G., Li, Y., Zhang, X., Xiong, Y., Huang, Q., Jin, S., 2022. Effects of the lignite bioorganic fertilizer on greenhouse gas emissions and pathways of nitrogen and carbon cycling in saline-sodic farmlands at Northwest China. J. Clean. Prod. 334, 130080.

Chen, Z., Sun, S., Zhu, Z., Chi, D., Huang, G., 2023. Modeling maize water consumption and growth under plastic film mulch using an agro–hydrological model: Searching for the optimal plant density in different hydrological years. Agric. Water Manag. 276, 108048.

Christy, B., Tausz-Posch, S., Tausz, M., Richards, R., Rebetzke, G., Condon, A., McLean, T., Fitzgerald, G., Bourgault, M., O'Leary, G., 2018. Benefits of increasing transpiration efficiency in wheat under elevated CO_2 for rainfed regions. Glob. Change Biol. 24 (5), 1965–1977.
Dutta, R., Chanda, K., Maity, R., 2022. Future of solar energy potential in a changing climate across the world: a CMIP6 multi-model ensemble analysis. Renew. Energ. 188, 819–829.
Gedney, N., Cox, P.M., Betts, R.A., Boucher, O., Huntingford, C., Stott, P.A., 2006. Detection of a direct carbon dioxide effect in continental river runoff records. Nature 439 (7078), 835–838.
Gong, W., Zhang, Y., Huang, X., Luan, S., 2013. High-resolution measurement of ammonia emissions from fertilization of vegetable and rice crops in the Pearl River Delta Region, China. Atmos. Environ. 65, 1–10.
Habib-Ur-Rahman, M., Ahmad, A., Raza, A., Hasnain, M.U., Alharby, H.F., Alzahrani, Y. M., Bamagoos, A.A., Hakeem, K.R., Ahmad, S., Nasim, W., Ali, S., Mansour, F., Sabagh, A.E., 2022. Impact of climate change on agricultural production; Issues, challenges, and opportunities in Asia. Front Plant Sci. 13, 925548.
Hatfield, J.L., Dold, C., 2019. Water-use efficiency: advances and challenges in a changing climate. Front Plant Sci. 10, 103.
Hayakawa, A., Akiyama, H., Sudo, S., Yagi, K., 2009. N_2O and NO emissions from an andisol field as influenced by pelleted poultry manure. Soil Biol. Biochem. 41, 521–529.
Huang, M., Wang, C., Qi, W., Zhang, Z., Xu, H., 2022. Modelling the integrated strategies of deficit irrigation, nitrogen fertilization, and biochar addition for winter wheat by AquaCrop based on a two-year field study. Field Crops Res 282, 108510.
Huang, Z., Xia, G., Hu, J., Chen, T., Zheng, J., Wu, Q., Chi, D., Wang, F., 2020. Optimization of mulched drip irrigation amount for peanut based on AHC model in northwestern Liaoning, China. J. Appl. Ecol. 31 (2), 483–492.
Igbadun, H.E., Salim, B.A., Tarimo, A.K.P.R., Mahoo, H.F., 2008. Effects of deficit irrigation scheduling on yields and soil water balance of irrigated maize. Irrig. Sci. 27 (1), 11–23.
IPCC, 2014. Climate Change 2014-mitigation of Climate Change: Working Group I Contribution to the Fourth Assessment Report of the IPCC. Cambridge University Press, Cambridge.
Kamran, M., Yan, Z., Ahmad, I., Jia, Q., Ghani, M.U., Chen, X., Chang, S., Li, T., Siddique, K.H.M., Fahad, S., Hou, F., 2023. Assessment of greenhouse gases emissions, global warming potential and net ecosystem economic benefits from wheat field with reduced irrigation and nitrogen management in an arid region of China. Agric. Ecosyst. Environ. 341, 108197.
Li, C., Xiong, Y., Cui, Z., Huang, Q., Xu, X., Han, W., Huang, G., 2020a. Effect of irrigation and fertilization regimes on grain yield, water and nitrogen productivity of mulching cultivated maize (Zea mays L.) in the Hetao Irrigation District of China. Agric. Water Manag. 232, 106065.
Li, C., Xiong, Y., Huang, Q., Xu, X., Huang, G., 2020b. Impact of irrigation and fertilization regimes on greenhouse gas emissions from soil of mulching cultivated maize (Zea mays L.) field in the upper reaches of Yellow River, China. J. Clean. Prod. 259, 120873.
Li, Y., Huang, G., Chen, Z., Xiong, Y., Huang, Q., Xu, X., Huo, Z., 2022a. Effects of irrigation and fertilization on grain yield, water and nitrogen dynamics and their use efficiency of spring wheat farmland in an arid agricultural watershed of Northwest China. Agric. Water Manag. 260, 107277.
Li, Y., Li, G., Chen, Z., Zhang, X., Huang, G., 2022b. Irrigation and N application strategies for spring wheat fields in the Hetao irrigation district based on N balance. Trans. CSAE 38 (17), 61–72.
Li, Y., Wang, R., Chen, Z., Xiong, Y., Huang, Q., Huang, G., 2023a. Increasing net ecosystem carbon budget and mitigating global warming potential with improved irrigation and nitrogen fertilization management of a spring wheat farmland system in arid Northwest China. Plant Soil 489, 193–209.
Li, Y., Xu, X., Chen, Z., Xiong, Y., Huang, Q., Huang, G., 2023b. A process simulation-based framework for resource, food, and ecology trade-off by optimizing irrigation and N management. J. Hydrol. 617, 129035.
Liu, D.L., Zuo, H., 2012. Statistical downscaling of daily climate variables for climate change impact assessment over New South Wales, Australia. Clim. Change 115 (3-4), 629–666.
Liu, M., Xu, X., Jiang, Y., Huang, Q., Huo, Z., Liu, L., Huang, G., 2020. Responses of crop growth and water productivity to climate change and agricultural water-saving in arid region. Sci. Total Environ. 703, 134621.
Liu, S., Wang, J.J., Tian, Z., Wang, X., Harrison, S., 2017. Ammonia and greenhouse gas emissions from a subtropical wheat field under different nitrogen fertilization strategies. J. Environ. Sci. 57, 196–210.
Lu, J., Bai, Z., Velthof, G.L., Wu, Z., Chadwick, D., Ma, L., 2019. Accumulation and leaching of nitrate in soils in wheat-maize production in China. Agric. Water Manag. 212, 407–415.
Mon, J., Bronson, K.F., Hunsaker, D.J., Thorp, K.R., White, J.W., French, A.N., 2016. Interactive effects of nitrogen fertilization and irrigation on grain yield, canopy temperature, and nitrogen use efficiency in overhead sprinkler-irrigated durum wheat. Field Crops Res 191, 54–65.
Nawaz, A., Ullah, A., Nadeem, F., Siddique, K., Farooq, M., 2022. Heat stress effects on the reproductive physiology and yield of wheat. J. Agron. Crop Sci. 208, 1–17.
O'Neill, B.C., Tebaldi, C., Vuuren, D.Pv, Eyring, V., Friedlingstein, P., Hurtt, G., Knutti, R., Kriegler, E., Lamarque, J.-F., Lowe, J., Meehl, G.A., Moss, R., Riahi, K., Sanderson, B.M., 2016. The Scenario Model Intercomparison Project (ScenarioMIP) for CMIP6. Geosci. Model Dev. 9 (9), 3461–3482.
Oertel, C., Matschullat, J., Zurba, K., Zimmermann, F., Erasmi, S., 2016. Greenhouse gas emissions from soils-a review. Geochemistry 76 (3), 327–352.
Parent, B., Leclere, M., Lacube, S., Semenov, M.A., Welcker, C., Martre, P., Tardieu, F., 2018. Maize yields over Europe may increase in spite of climate change, with an appropriate use of the genetic variability of flowering time. Proc. Natl. Acad. Sci. 115 (42), 10642–10647.
Patra, P.K., Canadell, J.G., Houghton, R.A., Piao, S.L., Oh, N.H., Ciais, P., Manjunath, K. R., Chhabra, A., Wang, T., Bhattacharya, T., Bousquet, P., Hartman, J., Ito, A., Mayorga, E., Niwa, Y., Raymond, P.A., Sarma, V.V.S.S., Lasco, R., 2013. The carbon budget of South Asia. Biogeosciences 10 (1), 513–527.
Rashid, M.A., Jabloun, M., Andersen, M.N., Zhang, X., Olesen, J.E., 2019. Climate change is expected to increase yield and water use efficiency of wheat in the North China Plain. Agric. Water Manag. 222, 193–203.
Ren, D., Xu, X., Hao, Y., Huang, G., 2016. Modeling and assessing field irrigation water use in a canal system of Hetao, upper Yellow River basin: Application to maize, sunflower and watermelon. J. Hydrol. 532, 122–139.
Riley, W.J., Ortiz-Monasterio, I., Matso, P.A., 2001. Nitrogen leaching and soil nitrate, nitrite, and ammonium levels under irrigated wheat in Northern Mexico. Nutr. Cycl. Agroecosyst. 61, 223–236.
Sainju, U.M., 2019. Improving nitrogen balance with irrigation practice and cropping system. J. Soil Water Conserv. 74 (6), 622–631.
Salo, T., Turtola, E., 2006. Nitrogen balance as an indicator of nitrogen leaching in Finland. Agric. Ecosyst. Environ. 113 (1-4), 98–107.
Scheer, C., Grace, P.R., Rowlings, D.W., Payero, J., 2012. Nitrous oxide emissions from irrigated wheat in Australia: impact of irrigation management. Plant Soil 359, 351–362.
Shi, Z., Li, D., Jing, Q., Cai, J., Jiang, D., Cao, W., Dai, T., 2012. Effects of nitrogen applications on soil nitrogen balance and nitrogen utilization of winter wheat in a rice–wheat rotation. Field Crops Res 127, 241–247.
Tan, L., Feng, P., Li, B., Huang, F., Liu, D.L., Ren, P., Liu, H., Srinivasan, R., Chen, Y., 2022. Climate change impacts on crop water productivity and net groundwater use under a double-cropping system with intensive irrigation in the Haihe River Basin, China. Agric. Water Manag. 266, 107560.
Tongwane, M.I., Moeletsi, M.E., 2018. A review of greenhouse gas emissions from the agriculture sector in Africa. Agric. Syst. 166, 124–134.
Trost, B., Prochnow, A., Meyer-Aurich, A., Drastig, K., Baumecker, M., Ellmer, F., 2016. Effects of irrigation and nitrogen fertilization on the greenhouse gas emissions of a cropping system on a sandy soil in northeast Germany. Eur. J. Agron. 81, 117–128.
Wand, S.J., Midgley, G.F., Jones, M.H., Curtis, P.S., 1999. Responses of wild C4 and C3 grass (Poaceae) species to elevated atmospheric CO_2 concentration: a meta-analytic test of current theories and perceptions. Glob. Change Biol. 5 (6), 723–741.
Wang, R., Huang, G., Xu, X., Ren, D., Gou, J., Wu, Z., 2022. Significant differences in agro-hydrological processes and water productivity between canal- and well-irrigated areas in an arid region. Agric. Water Manag. 267, 107637.
Wang, X., Li, L., Ding, Y., Xu, J., Wang, Y., Zhu, Y., Wang, X., Cai, H., 2021. Adaptation of winter wheat varieties and irrigation patterns under future climate change conditions in Northern China. Agric. Water Manag. 243, 106409.
Williams, J.R., Jones, C.A., Kiniry, J.R., Spanel, D.A., 1989. The EPIC crop growth model. Trans. ASAE 32 (2), 497–511.
Wu, Z., Li, Y., Wang, R., Xu, X., Ren, D., Huang, Q., Xiong, Y., Huang, G., 2023. Evaluation of irrigation water saving and salinity control practices of maize and sunflower in the upper Yellow River basin with an agro-hydrological model based method. Agric. Water Manag. 278, 108157.
Xu, X., Sun, C., Neng, F., Fu, J., Huang, G., 2018. AHC: An integrated numerical model for simulating agroecosystem processes—Model description and application. Ecol. Model. 390, 23–39.
Yang, Y., Li, N., Ni, X., Yu, L., Yang, Y., Wang, Q., Liu, J., Ye, Y., Tao, L., Liu, B., Wu, Y., 2019. Combining deep flooding and slow-release urea to reduce ammonia emission from rice fields. J. Clean. Prod. 244, 118745.
Zhang, H., Xiong, Y., Huang, G., Xu, X., Huang, Q., 2017. Effects of water stress on processing tomatoes yield, quality and water use efficiency with plastic mulched drip irrigation in sandy soil of the Hetao Irrigation District. Agric. Water Manag. 179, 205–214.
Zhang, X., Xiao, G., Bol, R., Wang, L., Zhuge, Y., Wu, W., Li, H., Meng, F., 2021. Influences of irrigation and fertilization on soil N cycle and losses from wheat-maize cropping system in northern China. Environ. Pollut. 278, 116852.
Zhang, Y., Feng, L., Wang, E., Wang, J., Li, B., 2012. Evaluation of the APSIM-Wheat model in terms of different cultivars, management regimes and environmental conditions. Can. J. Plant Sci. 92 (5), 937–949.
Zhou, L., 2020. Influences of deficit irrigation on soil water content distribution and spring wheat growth in Hetao Irrigation District, Inner Mongolia of China. Water Sci. Tech. -W. Sup. 20 (8), 3722–3729.
Zydelis, R., Weihermuller, L., Herbst, M., 2021. Future climate change will accelerate maize phenological development and increase yield in the nemoral climate. Sci. Total Environ. 784, 147175.